Progress In Electromagnetics Research, PIER 61, 39–65, 2006

BISAR MAPPING I. THEORY AND MODELLING

M. J. BenKassem and J. Saillard

IREENA – équipe Radar
Ecole Polytechnique de l'Université de Nantes
1 rue C. PAUC 44306 Nantes Cedex 03, France

A. Khenchaf

Centre de Recherche E3I2, ENSIETA
2 rue François Verny, 29806 Brest Cedex 09, France

Abstract—Bistatic Synthetic Aperture Radar (*BISAR*) is an active imaging system for which the transmitting and the receiving antennas are located on separate platforms. During its motion, the transmitting antenna emits towards the ground a burst of pulses at a frequency called Pulses Repetition Frequency. Every pulse affects an area of the ground after a propagation time proportional to the distance transmitter-scene. The bistatic receiving antenna receives a signal from the ground after a propagation time proportional to the distance scene-receiver. A communication link between the transmitter and the receiver is necessary to measure the phase of the received signal with respect to that of the transmitted signal.

This paper presents, initially, the modeling of a moving polarimetric radar working in bistatic configuration. We propose to write the received signal as a function of time for the general case where the transmitter, the target and the receiver are moving. As BISAR and MONOSAR (*Monostatic Synthetic Aperture Radar*) geometry differ substantially, the BISAR temporal requirements are examined in detail. The radiolink is completely modeled.

The companion paper is devoted to the development of two processing methods for bistatic radar imaging. Simulation and experimentation will be presented.

1. INTRODUCTION

Most of spaceborne active microwave missions have been carried out by a monostatic radar, which is a system with a single transmitting-receiving antenna.

Bistatic radar is one of main methods by which planetary surfaces can be mapped remotely. As illustrated in Fig. 1, in a conventional bistatic radar, the transmitter and receiver antennas are located on separate aircraft [1].

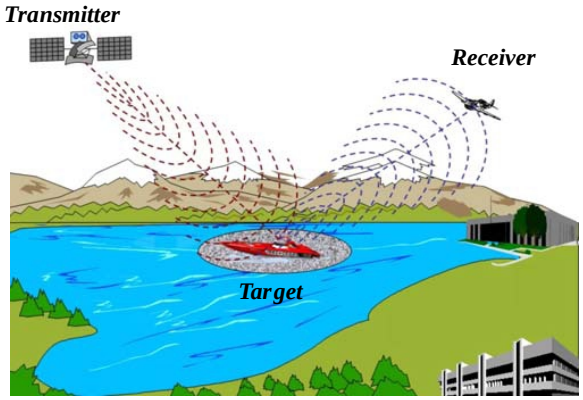

Figure 1. Geometric configuration.

Fundamental to bistatic investigation is the separation between the transmitter and the receiver, which allows the closest characterisation of target scattering properties. Some of these target properties may not be apparent from, or easily interpreted using, monostatic observations. Technological progress enabled the placement of the transmitter and the receiver aboard satellites, ships, planes or other carriers. Because of the delocalisation of the transmitter and receiver, it is possible to improve the capacity of the radar detection and identification, and thus to increase the detection capability of a furtive target. Furthermore, with two images of the same area viewed from different angles, it is possible to obtain three dimensional stereo images.

Modern radar requires sophisticated signal processing techniques to obtain better resolution and excellent detection capabilities. That is dictated by new missions assigned to radar. In point of fact, they do not only carry out target detection and localisation, but they are also used to identify the target [2]. The use of a new kind of system such as polarimetric radars developed in a bistatic configuration gives additional information on the detected target, improving its

identification. Furthermore, this type of radar tends to reduce the efficiency of furtivity and jamming techniques. Polarimetric bistatic radar yields a great advantage for detection of targets embedded in a perturbed environment, as is the case in a natural media or in an electronic ware fare context [3].

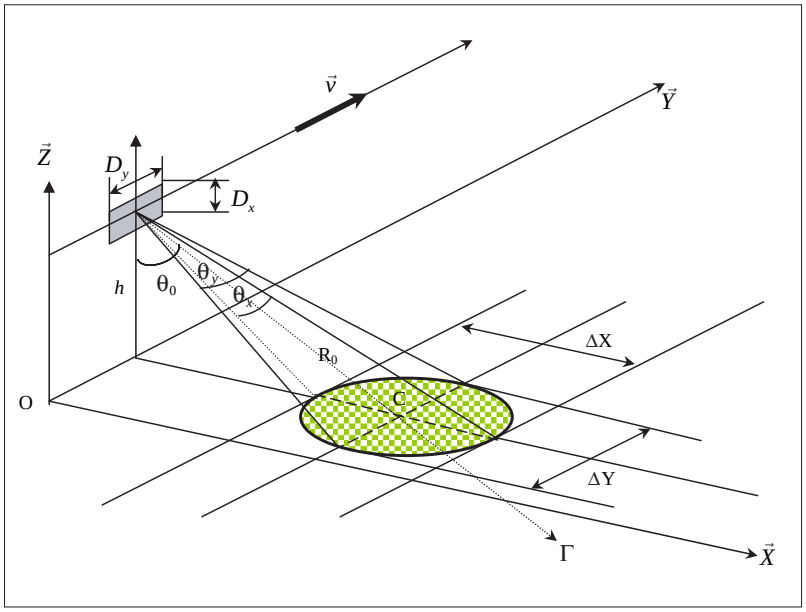

Figure 2. Geometric configuration of a monostatic SAR.

Synthetic Aperture Radar SAR (Fig. 2) is an echo-mode array imaging system. Similar to the other array imaging systems, SAR provides a multidimensional database that can be manipulated via signal processing means to obtain a multidimensional image that carries information on the target area under study. The signal subspace of the acquired data is formed by varying the radar frequency and radiation pattern in the target area [5]. Thus the SAR is an airborne or satellite-borne radar system that provides high resolution maps of remote targets on a terrain, or a planet. SAR systems are a highly developed combination of precision hardware and electronic design for data acquisition, and advanced theoretical principle of mathematics and physics to convert the acquired data to a high resolution image [5].

SAR supplies images based on the waves reflected by the earth surface. This technique is very useful since it doesn't depend on the weather conditions. It reveals properties of the earth's surface that do

not appear on classical optical images [6]. Indeed, radar waves may, for example, describe drifted ices on sea; they can penetrate under vegetation and even slightly into the basement. However, the main problem with this approach is the interpretation of the radar image that is different from usual optical ones.

A synthetic aperture radar which operates with one antenna to transmit and receive the radar signal is called a monostatic SAR or *MONOSAR*. The antenna is shared at time between the functions of transmission and reception. Fig. 2 shows the strip map monostatic SAR geometry and radar position relative to the ground. A burst of pulses is transmitted by a side looking antenna pointed towards the ground and the backscattered power is collected with the signal corresponding to each pulse. The SAR system saves the phase histories of the responses at each position as the real beam moves past and then, in post processing it evaluates, phase shifts and sums them up to focus on one point target (*resolution element*) at a time and suppresses all the others.

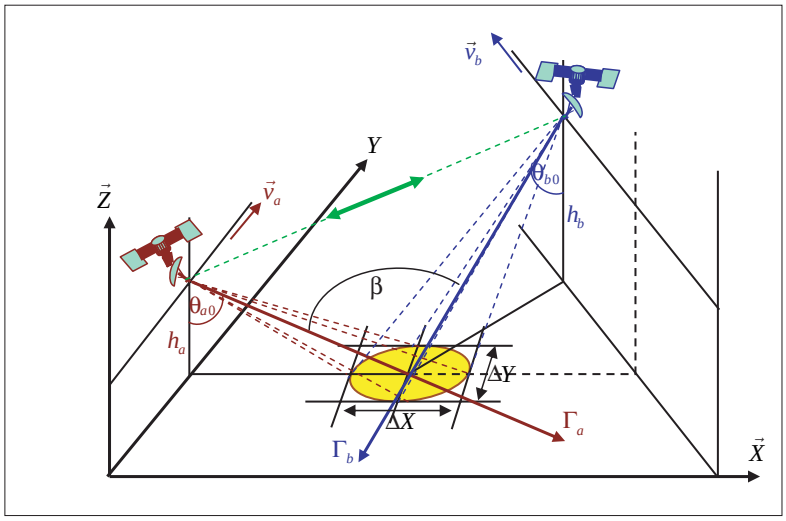

Figure 3. Geometrical configuration of a bistatic SAR.

A SAR can be designed in order to operate with two separate antennas to perform the transmitted and received functions and it is called Bistatic SAR or *BISAR* [3]. A radar system is said to be in bistatic configuration (Fig. 3) when the transmitter and the receiver are located on separate aircraft [7]. A communication link between the transmitter and the receiver is necessary to measure the phase of the received signal relative to that of the transmitted signal [8, 9]. We

assumed that the direction of the two narrow beams is programmed to coincide over the desired area to be imaged. The transmitter and receiver portions can be interchanged. There may be advantages in having particular antennas on specific platforms for operational reasons.

Radar images of the earth surface can be produced with a BISAR. With two images of the same area viewed from different angles, it is possible, for example, to reveal shadow zones which do not appear in monostatic SAR, to enhance system detection and resolution especially for dissymmetric targets or for any class reflectors. Moreover it is also possible to derive three-dimensional stereo images. Finally for the same resolution, the amount of integration time and transmitter power is less than those required for a monostatic SAR [4].

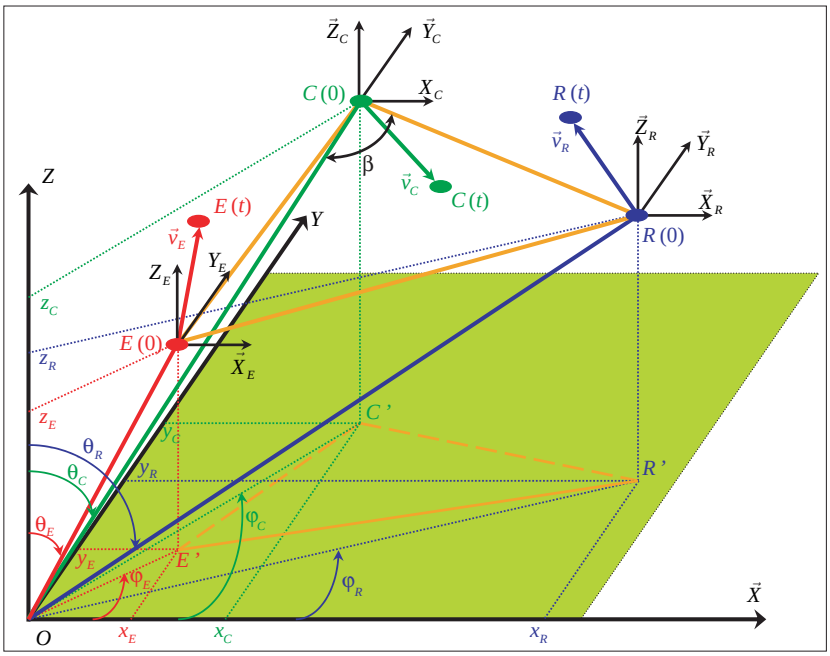

Figure 4. Geometry of a bistatic connection.

2. MODELLING FOR BISAR CONNECTION

The general geometry of a bistatic radiolink between a moving transmitter, a moving target and a moving receiver is illustrated on Fig. 4. The distance separating the transmitter, the target and the receiver positions vary with time as function of the mobile velocity.

Velocity vectors are respectively noted $\vec{v}_E(t)$, $\vec{v}_C(t)$ and $\vec{v}_R(t)$. The instantaneous location of the transmitter, the target, and the receiver is computed from their velocity and their initial location defined by the height over the earth surface, the latitude angle and the longitude angle. The mobiles velocity is provided in a vectorial formulation by its three projections on the height, the north direction, and the east direction. The Doppler phenomena is included in the calculation of the received waveform by the time variation of the propagation delay between the transmitter and the receiver depending on the target and radar platforms locations and velocities [7].

Amplitude and phase of the signal collected at the receiving antenna depends also on the target and the polarisation of the transmitted electromagnetic wave. The target polarimetric behaviour is provided using its coherent scattering matrix $[S]$ [10]. This matrix also called the Sinclair matrix is 2×2 complex matrix relating the Jones vectors of the transmitting wave and the receiving wave. Thus it is completely defined by eight real parameters. However, in practice, only seven parameters are considered (*four modules and three relative phases*). The coefficients of the scattering matrix depend on the geometrical and physical features of the target. They also depend on the target observation angles that are on the location of the transmitter and the receiver compared with the target.

The propagation delay between the transmission and reception of the wave emitted at the time t is equal to propagation time Δt_{ER} of the wave between the transmitter and the receiver passing by the target.

Assume that the incident wave is reflected instantly by the target, the propagation time between the transmitter and the receiver will be the sum of the propagation times between the transmitter and the target and the propagation time between the target and the receiver [5].

$$\Delta t_{ER}(t) = \Delta t_{EC}(t) + \Delta t_{CR}(t) \tag{1}$$

$\Delta t_{EC}(t)$ is the propagation time delay between the transmitter and the target; it is given by (2).

$$\Delta t_{EC}(t) = \frac{\vec{E}_t\vec{C}_t \cdot \vec{V}_C(t) + \sqrt{\left\|\vec{E}_t\vec{C}_t \cdot \vec{V}_C(t)\right\|^2 + \left\|\vec{E}_t\vec{C}_t\right\|^2 \left(c^2 - \left\|\vec{V}_C(t)\right\|^2\right)}}{c^2 - \left\|\vec{V}_C(t)\right\|^2} \tag{2}$$

$\vec{E}_t\vec{C}_t$ is the vector which connects the transmitter and the target at

time t, $\vec{V}_C(t)$ is the target velocity vector, c is the celerity of the electromagnetic wave ($c = 3 \cdot 10^8$).

$\Delta t_{CR}(t)$ is the propagation time delay between the target and the receiver; it is given by (3).

$$\Delta t_{CR}(t) = \frac{\vec{C}_{t_C}\vec{R}_{t_C} \cdot \vec{V}_r(t) + \sqrt{\left\|\vec{C}_{t_C}\vec{R}_{t_C} \cdot \vec{V}_r(t)\right\|^2 + \left\|\vec{C}_{t_C}\vec{R}_{t_C}\right\|^2 \left(c^2 - \left\|\vec{V}_r(t)\right\|^2\right)}}{c^2 - \left\|\vec{V}_r(t)\right\|^2} \tag{3}$$

t_C is the arrival time of the wave at the target, $\vec{C}_{t_C}\vec{R}_{t_C}$ is the vector connecting the target and the receiver at time t_C, $\vec{V}_r(t)$ is the receiver velocity vector.

If the communication between the transmitter and the receiver can be done by a direct way, then the direct propagation time of the signal between the transmitter and the receiver is given by (4).

$$\Delta t_{ER}(t) = \frac{\vec{E}_t\vec{R}_t \cdot \vec{V}_r(t) + \sqrt{\left\|\vec{E}_t\vec{R}_t \cdot \vec{V}_r(t)\right\|^2 + \left\|\vec{E}_t\vec{R}_t\right\|^2 \left(c^2 - \left\|\vec{V}_r(t)\right\|^2\right)}}{c^2 - \left\|\vec{V}_r(t)\right\|^2} \tag{4}$$

$\vec{E}_t\vec{R}_t$ is the vector link between the transmitter and the receiver at time t.

It is assumed the transmitter, the target and the receiver are stationary during one slot time of transmitting-receiving.

The temporal variation of the propagation delay modifies the received signal with respect to the transmitted signal. The temporal characteristics of the pulsed transmitted and received signals governed the functional operation of a SAR, such as range ambiguity, azimuth ambiguity, resolution and data processing. Inasmuch as the BISAR and MONOSAR geometries differ substantially, the BISAR temporal requirements are examined in detail. Therefore, analysis of the equidistance and equidoppler surfaces yield information about the target position.

3. EQUIDISTANCE AND EQUIDOPPLER SURFACES

Synthetic aperture radar is a microwave imagery system able to produce high resolution image by processing properly data collected by a relatively small antenna.

High range resolution image is achieved through traditional pulse compression methods. This treatment depends only on frequency modulation rate which is known for a given system.

High cross range resolution is accomplished by moving the physical antenna position as a function of time, and coherently processing the echoes received during the time taken to through the synthetic aperture radar length.

The processing in the cross range direction requires preliminary estimation of the Doppler parameters. Indeed, the use of the information referred to the Doppler effect affecting the frequency of the diffused waves makes it possible to have the best cross range resolution. It is a question of separating the contribution of the mapped surface elements at the time of their crossing by the lobe of the antennae. The purpose of the Doppler shift analysis is to look for the information which corresponds to a given pixel of the surface that we desire to take in image when the bistatic connection is moving. Thus, it is essential to estimate the Doppler frequency for a given configuration of the bistatic connection.

3.1. Equidistance Surfaces

In MONOSAR, range is measured in terms of time delay. This is convenient because of the use of a single antenna to transmit and receive the wave. In this case, the equidistance surfaces are the space points sets which are at the same distance from the transmitting receiving antenna. Equidistance surfaces in MONOSAR case are spheres in space. Then the intersections with the supposed plane ground surface, are circles (Fig. 5).

In BISAR the equivalent entity are surfaces of constant time delay between the transmitter and the receiver. Equidistance in BISAR case are ellipsoids in space and ellipses in the bistatic plane (*plane containing the transmitter, the receiver, and the target*) and on the surface of the ground, supposed plane (Fig. 6).

3.2. Equidoppler Surfaces

In MONOSAR, the velocity is equivalent to Doppler shift and it is derived from constant Doppler frequency surfaces called equidopplers (Fig. 7) [4]. Equidoppler surfaces are the space point's sets which appear at the same Doppler frequency shift.

In BISAR, equidoppler surfaces are computed from the sum of the Doppler effect of the moving transmitting antenna, the moving receiving antenna, and the moving target.

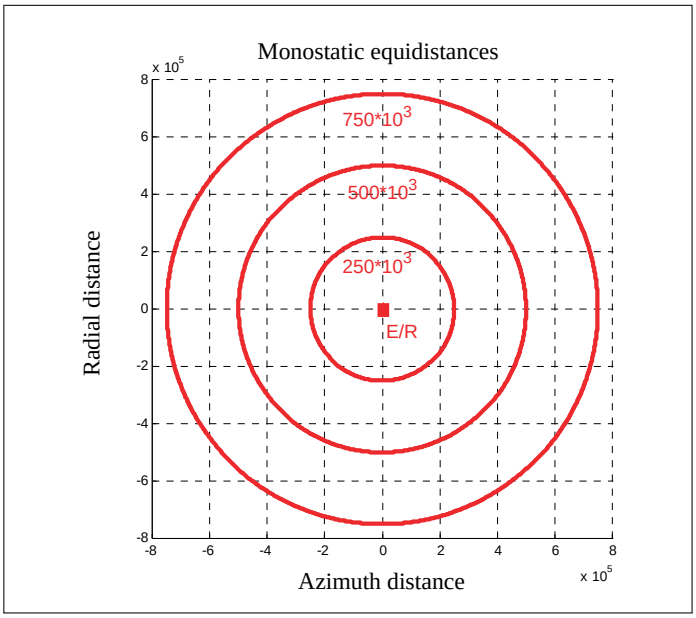

Figure 5. Monostatic equidistance contours.

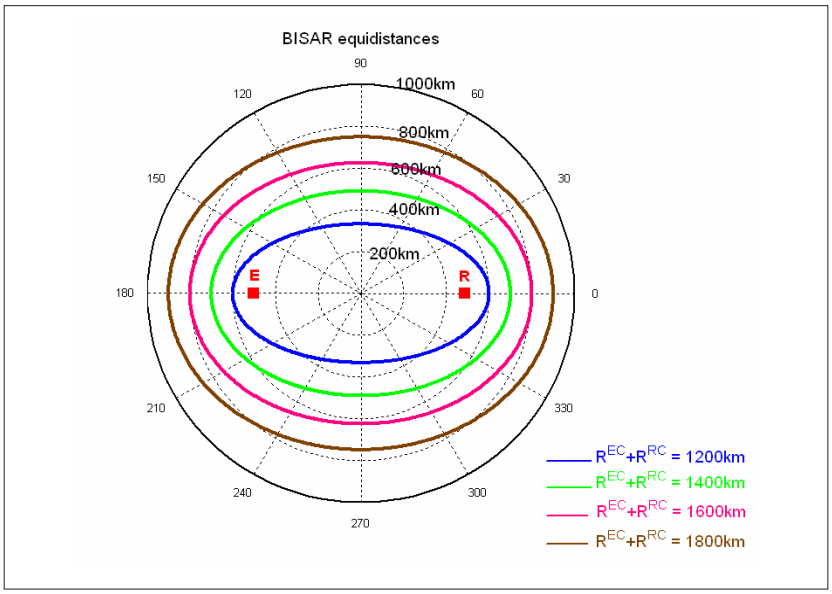

Figure 6. Bistatic equidistance contours in the bistatic plane.

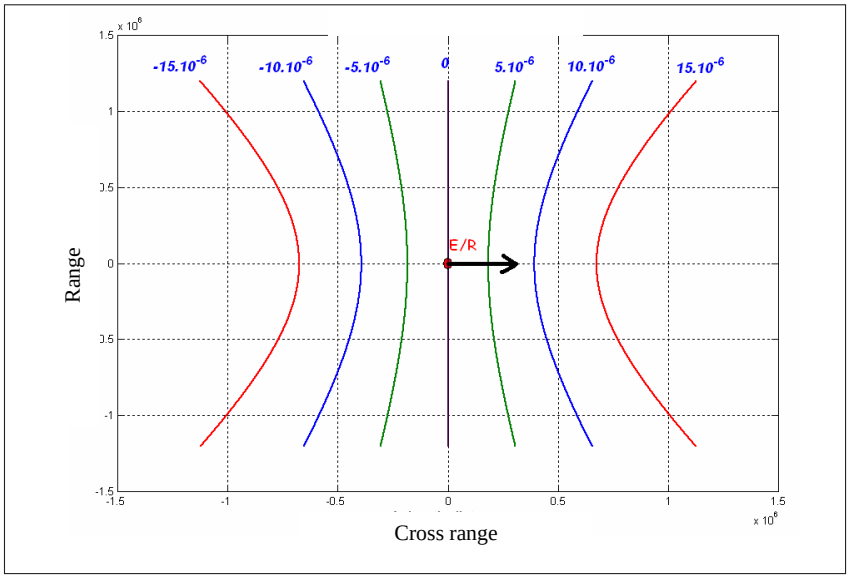

Figure 7. Normalized monostatic equidoppler contours.

A signal emitted at the frequency f_0 by a radar embarked on board of a moving platform will appear for a ground observer like a signal at the frequency f_1. such as:

$$f_1 = f_0 + f_d \tag{5}$$

Where f_d is the Doppler frequency shift due to the displacement of the platform.

In monostatic configuration, the intersections of the equidoppler surfaces with the supposed plane ground surface are hyperbolas (Fig. 7).

As previously mentioned, when the signal is emitted from one antenna and received by another antenna separated by a large distance as for bistatic systems, the equidopplers are computed from the sum of the Doppler effect of the transmitter, the receiver and the target.

In the instantaneous bistatic plane Fig. 8, the Doppler frequency due to the displacement of the transmitter, the target and the receiver is given by (6)

$$f_d = \frac{2V_C}{\lambda}\cos(\alpha)\cos\left(\frac{\beta}{2}\right) + \frac{V_E}{\lambda}\cos(\alpha_E - \theta_E) + \frac{V_R}{\lambda}\cos(\alpha_R - \theta_R) \tag{6}$$

Where β is the bistatic angle (*angle between the transmitter and receiver with vertex at the target*).

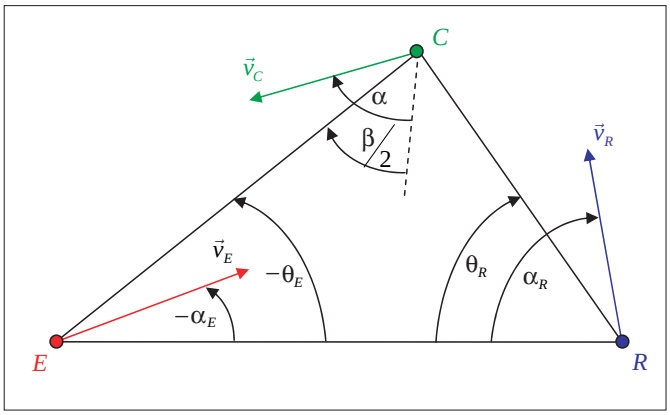

Figure 8. Bistatic equidoppler geometry.

The target's velocity vector projected onto the bistatic plane has magnitude $\vec{V}_C$ and aspect angle α referenced to the bistatic bisector. The aspect angle is positive when measured clockwise from the bistatic bisector. The transmitter and the receiver have projected velocity vectors of magnitude $\vec{V}_E$ and $\vec{V}_R$, and aspect angles α_E and α_R, respectively, referenced to the baseline [ER].

Aspect angles are positive when measured clockwise from the baseline [ER].

θ_E is the transmitter look angle in the bistatic plane. It is related to the transmitter azimuth angle θ_{Ea} and transmitter elevation angle θ_{Ed} as shown in (Fig. 9) by:

$$\theta_E = \cos^{-1}(\cos(\theta_{Ea})\cos(\theta_{Ed})) \tag{7}$$

θ_R is the receiver look angle in the bistatic plane. It is related to the receiver azimuth angle θ_{Ra} and receiver elevation angle θ_{Rd} as shown in (Fig. 9) by:

$$\theta_R = \cos^{-1}(\cos(\theta_{Ra})\cos(\theta_{Rd})) \tag{8}$$

Various configurations of bistatic radar connection are possible. The nature of equidoppler surfaces depends on the chosen geometrical configuration.

Fig. 10 shows equidistance and equidoppler contours in the bistatic system case for which the transmitter and the receiver are moving on two parallel trajectories. Equidistance contours are ellipses and equidoppler contours are hyperbolas for the transmitter and the receiver. In this case, the bistatic equidopplers are also hyperbolas.

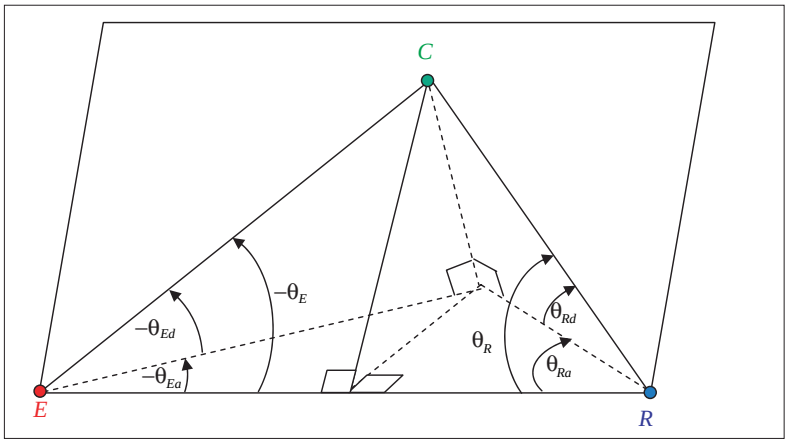

Figure 9. Geometry to compute look angles according to azimuth and elevation angles.

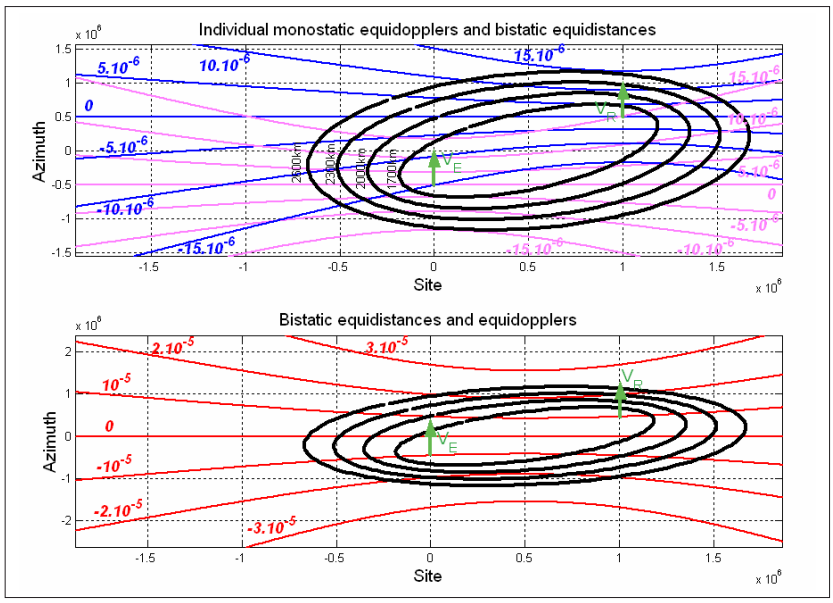

Figure 10. Bistatic equidistance contours and normalized bistatic equidoppler contours when the transmitter and the receiver are moving on two parallel trajectories.

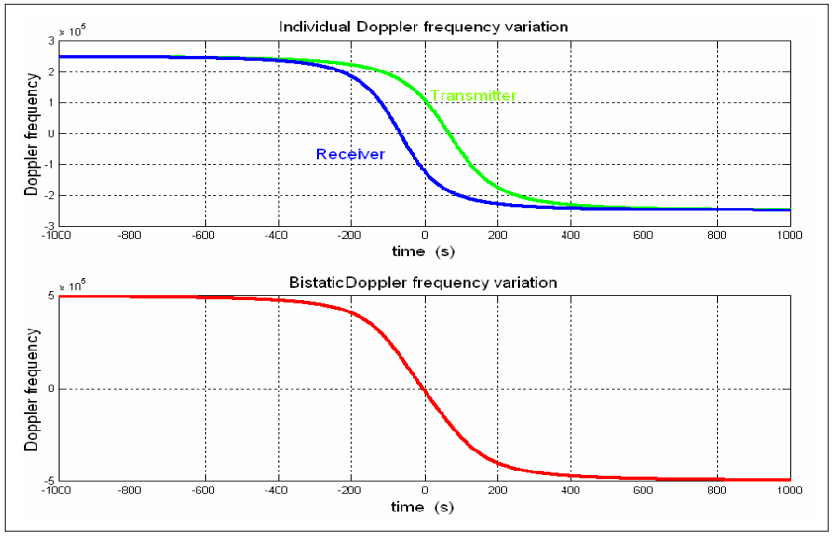

Figure 11. Doppler frequency variation for one pixel.

It is supposed that the earth rotation is negligible in this case. It is also assumed that the transmitter and the receiver move in parallel trajectory, in the same direction at 7,5 km/s, separated by $X_0 = 1000$ km in the range direction and by $Y_0 = 1000$ km in the cross range direction. The transmitting and the receiving antennas are at the same height $h_E = h_R = 900$ km.

For the same geometrical configuration, Fig. 11 shows the Doppler frequency variation of the same pixel according to time [12].

Equidoppler contours are shown in Figure 12, in the general case for which, both trajectory of the transmitting antenna situated at the altitude $h_E = 900$ km and the receiving antenna situated at the altitude $h_R = 900$ km form an angle $\alpha = \frac{\pi}{4}$.

The Doppler frequency variation of the same pixel according to time in this geometrical configuration case is shown in Fig. 13.

Finally, Fig. 14 shows, in the plane, equidistance and equidoppler contours in the monostatic system case. Equidistance contours are circles and equidopplers contours are hyperbolas. In this case, it is necessary to note that all pixels located at the same distance are detected for the same signal to noise ratio. This property is not valid in the case of the bistatic system. This difference between the monostatic and the bistatic systems requires the study of the bistatic signal to noise ratio variation. This difference will be detailed in the following section.

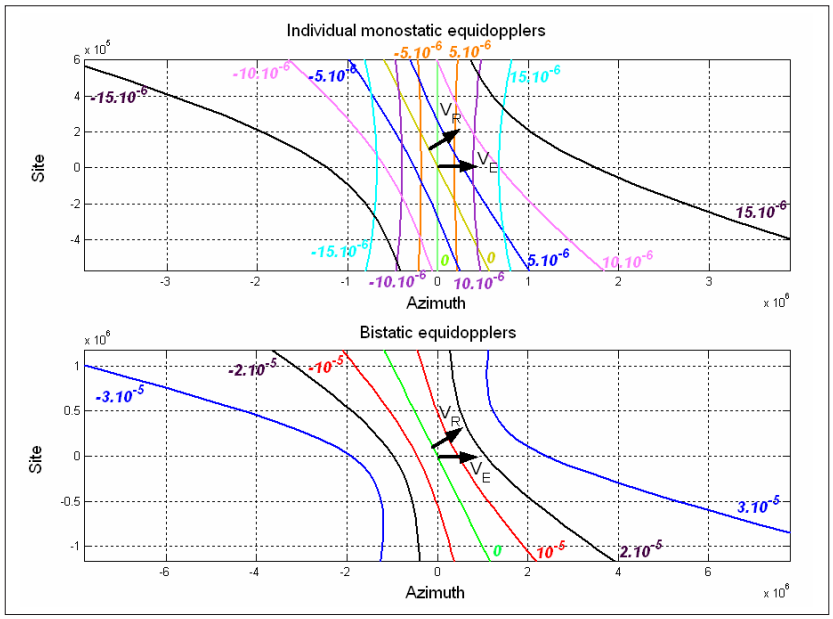

Figure 12. Normalized bistatic equidoppler contours (for $\alpha = \frac{\pi}{4}$).

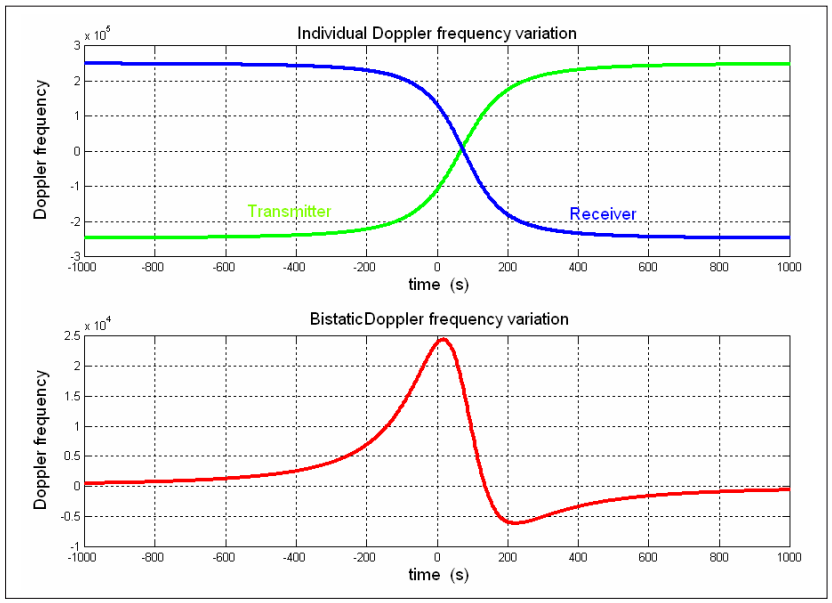

Figure 13. Doppler frequency variation.

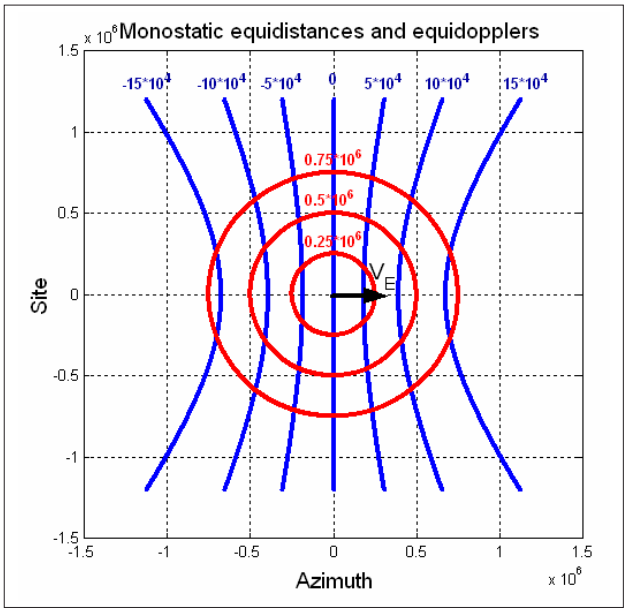

Figure 14. Monostatic equidistance contours and normalized equidoppler contours.

4. BISTATIC SIGNAL TO NOISE RATIO (*BSNR*)

The main problem of the radar is the recognition of a signal coming from a target when it is mixed with noise.

If the target observed by the radar does not emit any interfering signal, and if the radar is not subjected to artificial jamming, the bistatic signal to noise ratio (*BSNR*) at the exit of the receiving antenna can be written as:

$$BSNR = \frac{P_E G_E G_R \lambda^2 \sigma_b F_E^2 F_R^2}{(4\pi)^3 R_E^2 R_R^2 K T_S B_n L_E L_R L_S} \tag{9}$$

where:

P_E is the transmitter signal power,
G_E is the transmitting antenna gain,
G_R is the receiving antenna gain,
λ is the wavelength.
σ_b is the bistatic radar cross section (*RCS*),

F_E is the pattern propagation factor for transmitter to target path,
F_R is the pattern propagation factor for target to receiver path,
R_E is the transmitter to target distance,
R_R is the receiver to target distance,
K is the Boltzmann's constant,
T_S is the receiving system noise temperature,
B_n is the noise bandwidth of receiver's predetection filter,
L_E are the transmitting systems losses,
L_R are the receiving systems losses,
L_S is the system loss,

Equation (9) can be related to the corresponding monostatic equation by letting:

$$G^2 = G_E G_R, \quad \sigma_m = \sigma_b, \quad R^2 = R_E R_R, \quad \text{and} \quad L^2 = L_E L_R.$$

The peak power requirement can be reduced by using pulse compression techniques, and a signal to noise improvement can be derived from pulse integration associated with coherent signal processing. The bistatic radar cross section σ_b is generally greater than the monostatic radar cross section of the same surface [7].

From (9), we can determine the range of the bistatic radar such as

$$R_E R_R = \sqrt{\frac{k}{(BSNR)}} \tag{10}$$

where

$$k = \frac{P_E G_E G_R \lambda^2 \sigma_b F_E^2 F_R^2}{(4\pi)^3 K T_S B_n L_E L_R L_S} \tag{11}$$

From (10) we note that for an increasing $R_E R_R$, the bistatic signal to noise ration is reached for a minimal value. But this is with the detriment of the detection probability which increases with BSNR. A judicious compromise must be carried out in order to obtain a large enough bistatic range for a sufficient detection probability at one time.

Expression (10) which gives bistatic radar range is similar in form to the monostatic range expression. The principal difference is that $R_E R_R$ replaces R^2. This simple difference causes significant differences in monostatic and bistatic radar operation conditions [3].

One major difference is that level contours for a constant BSNR are defined by ovals of Cassini, rather than by circles for the simplest

monostatic case. These ovals are particularly useful in defining regions where the bistatic radar can operate.

A convenient way to plot ovals of Cassini is in polar coordinate system (r, θ) as shown in (Fig. 15).

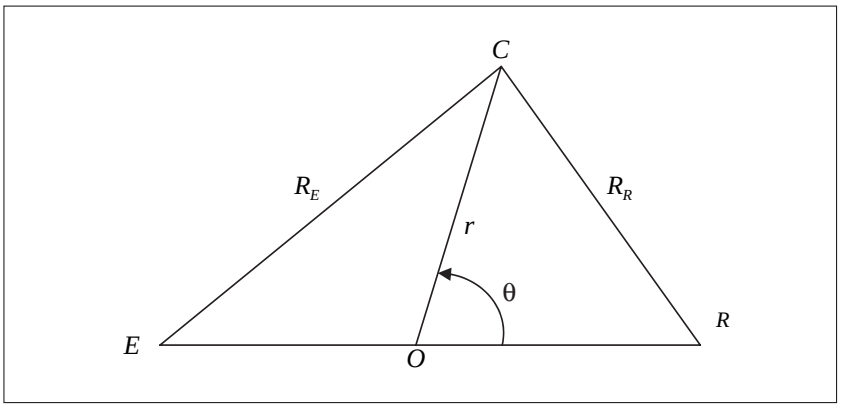

Figure 15. Polar geometry.

Converting $R_E R_R$ to polar coordinates yields

$$r = A\sqrt{\cos(2\theta) \pm \sqrt{\left(\frac{B}{A}\right)^4 - \sin^2(2\theta)}} \tag{12}$$

Where

$$A = \frac{L}{2} \tag{13}$$

And

$$B = \sqrt[4]{\frac{k}{BSNR}} \tag{14}$$

Equation (12) is plotted in bistatic plane for different values of BSNR. k is taken equal to $40L^4$. It is assumed that k is invariant with r and θ, which is usually not the case.

Ovals of Cassini, showed in (Fig. 16) define four distinct operating regions for bistatic radar.

a. Area near receiving system, the small oval around the receiver. This region occurs when $L > 2B$ and $R_E \gg R_R$.

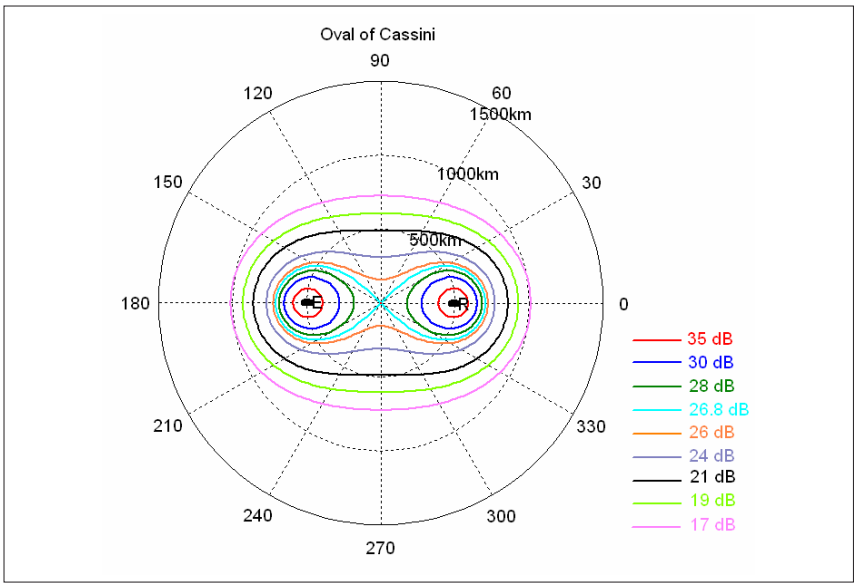

Figure 16. Ovals of Cassini.

b. Area near transmitting system, the small oval around the transmitter. This region occurs when $L > 2B$ and $R_R \gg R_E$.
c. Medium area system or transmitter-receiver centred area, the ovals surrounding both transmitter and receiver. This region occurs when $L < 2B$.
d. For $L = 2B$, the oval of Cassini is called a Bernoulli lemniscate. The point on the baseline where the oval breaks into two parts is called the cusp.

A second difference is that bistatic constant range sum contours, defined by $R_E + R_R$ are ellipses, and are not collinear with bistatic constant detection contours defined by ovals of Cassini ; whereas for the monostatic case they are both collinear circles. This difference sets operating limits for the bistatic radar, and also causes the BSNR to vary as a function of target position on a constant range sum contour.

Fig. 17 shows the variation which the BSNR must undergo to detect the various targets located at the same time delay between the transmitter and the receiver (*equidistance contour*).

Thus, targets A, B, C, D, F, G, H, and I are located on the same equidistance ellipse. This ellipse checks (15).

$$EM + MR = 1600\,\text{km} \tag{15}$$

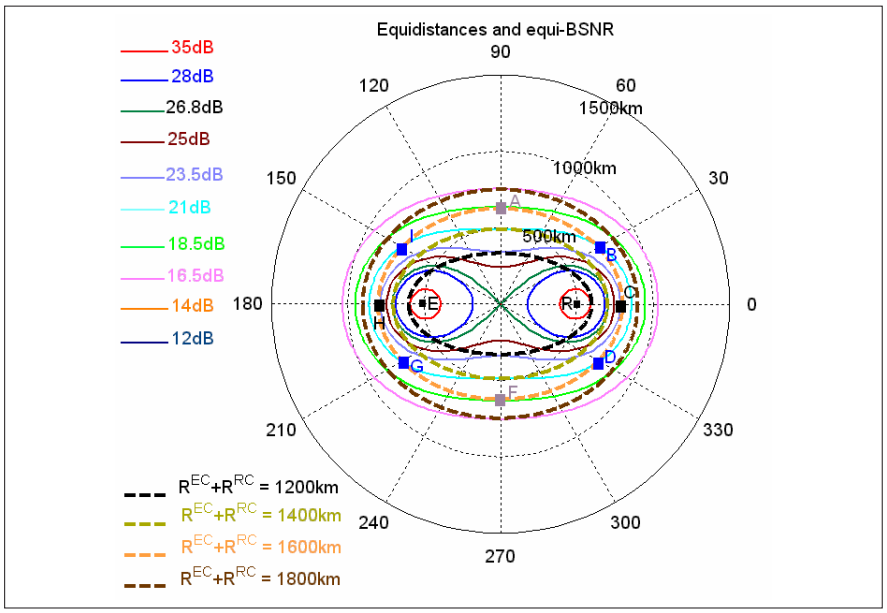

Figure 17. Variation of the BSNR to detect pixels located on the same equidistance surface.

Where

$$M = (A, B, C, D, F, G, H, I) \tag{16}$$

Pixels A and F are detected for BSNR = 18.5 dB

Pixels B, D, G and I are detected for BSNR = 21 dB

Pixels C and H are detected for SNR = 23.5 dB

Therefore, to detect all pixels located on the same time delay between the transmitter and the receiver, it is necessary to consider a floating BSNR between the two value $BSNR_{\min}$ and $BSNR_{\max}$.

The $BSNR_{\min}$ value corresponds to the $BSNR$ necessary and sufficient to detect pixels situated at the intersection of the mid-perpendicular of the baseline $[ER]$ with the equidistance ellipse.

The $BSNR_{\max}$ value corresponds to the $BSNR$ necessary and sufficient to detect pixels situated in the ellipse apogee and perigee.

The advantage is that the variation of the $BSNR$ could be used to discriminate the targets which are seen for the same delay between the transmitter and the receiver but which will differ by the $BSNR$ of their detection.

5. BISTATIC SYNTHETIC APERTURE RADAR CONFIGURATION

In this section, we chose a configuration for which the transmitter and the receiver move in parallel trajectory to observe the scene, (Fig. 18). The scene consists of a whole of isotropic elementary contributors.

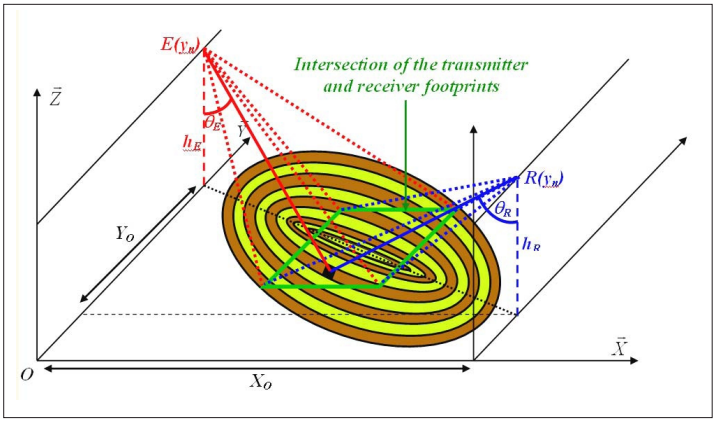

Figure 18. Configuration for bistatic mapping.

It is supposed that the two the transmitter and the receiver are separate in range direction by a distance equal to X_0 and in cross range direction by a distance equal to Y_0.

The illuminated zone is defined by the aperture angles θ_{Ea} in cross range direction and θ_{Ed} in range direction of the transmitting antenna lobe, and by its angle toward the vertical reference θ_{E0}.

The aperture of the transmitting antenna lobe is defined by:

$$\theta_{Ea} = \frac{\lambda_0}{L_E} \tag{17}$$

$$\theta_{Ed} = \frac{\lambda_0}{H_E} \tag{18}$$

L_E is the length of the transmitting antenna,

H_E is the width of the transmitting antenna,

λ_0 is the wavelength.

The transmitting antenna is located at a height h_E, moving at a velocity $\vec{v}_E$, along the azimuth axis Y, (Fig. 18).

In the orthonormal set $O(\vec{i}, \vec{j}, \vec{k})$, coordinates of the transmitting radar are $E \begin{pmatrix} 0 \\ y^E \\ h_E \end{pmatrix}$.

The zone illuminated by the transmitting radar is defined by (19) and (20).

$$h_E \tan(\theta_{E0}) - \frac{\Delta X_E}{2} \leq x \leq h_E \tan(\theta_{E0}) + \frac{\Delta X_E}{2} \tag{19}$$

$$y^E - \frac{\Delta Y_E}{2} \leq y \leq y^E + \frac{\Delta Y_E}{2} \tag{20}$$

Where

$$\Delta X_E = \frac{h_E \lambda_0}{H_E \cos^2(\theta_{E0})} \tag{21}$$

$$\Delta Y_E = \frac{h_E \lambda_0}{L_E \cos(\theta_{E0})} \tag{22}$$

The zone viewed by the receiving antenna is also defined by the aperture angles θ_{Ra} in cross range direction and θ_{Rd} in range direction of the receiving antenna lobe, and by its angle toward the vertical reference θ_{R0}.

The aperture of the receiving antenna lobe is defined by (23) and (24):

$$\theta_{Ra} = \frac{\lambda_0}{L_R} \tag{23}$$

$$\theta_{Rd} = \frac{\lambda_0}{H_R} \tag{24}$$

L_R is the length of the receiving antenna,

H_R is the width of the receiving antenna,

The receiving antenna is located at a height h_R, moving at a velocity $\vec{v}_R$, along the azimuth axis Y (Fig. 18).

The coordinates of the receiving radar are $R \begin{pmatrix} X_0 \\ y^R \\ h_R \end{pmatrix}$.

The zone viewed by the receiving antenna is defined by (25) and (26).

$$X_0 - h_R \tan(\theta_{R0}) - \frac{\Delta X_R}{2} \leq x \leq X_0 - h_R \tan(\theta_{R0}) + \frac{\Delta X_R}{2} \tag{25}$$

$$y^R - \frac{\Delta Y_R}{2} \leq y \leq y^R + \frac{\Delta Y_R}{2} \tag{26}$$

Where

$$\Delta X_R = \frac{h_R \lambda_0}{H_R \cos^2(\theta_{R0})} \tag{27}$$

$$\Delta Y_R = \frac{h_R \lambda_0}{L_R \cos(\theta_{R0})} \tag{28}$$

Thus, for the configuration suggested, (Fig. 18), the defined by the intersection of the transmitter lobe footprint and the receiver lobe footprint check (29) and (30)

$$X_0 - h_R \tan(\theta_{R0}) - \frac{\Delta X_R}{2} \leq x_M \leq h_E \tan(\theta_{E0}) + \frac{\Delta X_E}{2} \tag{29}$$

$$y^E - \frac{\Delta Y_E}{2} \leq y_M \leq y^R + \frac{\Delta Y_R}{2} \tag{30}$$

6. TRANSMITTED ELECTROMAGNETIC FIELD

The choice of the transmitted signal has a great influence on the detection capability and on the resolving power of the radar. In this way, the use of the pulse compression techniques gives good resolution both in distance and Doppler frequency [10, 12, 13]. These techniques are based on a bandwidth widening. This is accomplished by modulating the transmitted pulse either in phase or in frequency, and provides a finer-range resolution than can be achieved with a conventional radar system using an unmodulated pulse. Pulse compression technique is realized in our algorithm by adopting the chirp technique [14]. Thus, the frequency of transmitted pulse is linearly swept from $f_0 - \frac{\Delta f}{2}$ to $f_0 + \frac{\Delta f}{2}$. The time variation of the frequency is given by (31) as a function of the carrier frequency f_0, the transmitted bandwidth Δf, and the pulse duration T_i [15].

$$f(t) = f_0 + \frac{\Delta f}{T_i}\left(t - \frac{T_i}{2}\right) \tag{31}$$

Writing the pulse repetition rate T_r, the expression of the transmitted wave form is given by (32)

$$S_e(t) = \sum_{n=0}^{\infty} \mathrm{Re}\, ct_T(t - nT_r) e^{j2\pi(t-nT_r)f_0} e^{j2\pi(t-nT_r)\frac{\Delta f}{2T_i}[t-(n+\alpha)T_r]} \tag{32}$$

Where f_0 is the carrier frequency,
T_i is the duration of the pulse,

T_r is the pulse repetition rate,
$\alpha = \frac{T_i}{T_r}$ is the cyclic burst of pulse report,
Δf is the transmitted bandwidth.
The transmitted waveform is drawn in (Fig. 19) considering a rectangular pulse shape.

7. EXPRESSION OF THE RECEIVED SIGNAL

The transmitting antenna and the receiving antenna for a BISAR are embarked on separate sensors. During its move (Fig. 17), the transmitting antenna emits a burst of pulses towards the ground. Every pulse affects a pixel of the ground after a propagation times $\Delta t_{EC}(t)$ proportional to the distance transmitter-scene. The bistatic receiving antenna receives a signal from all the present reflectors in the common lobe of the transmitting antenna and the receiving antenna.

The bloc diagram Fig. 20 illustrates the receiving signal processing for image reconstruction.

The BISAR is thus an imagery system which allows a radar image with a high resolution.

The received electric field at the receiving antenna is obtained as

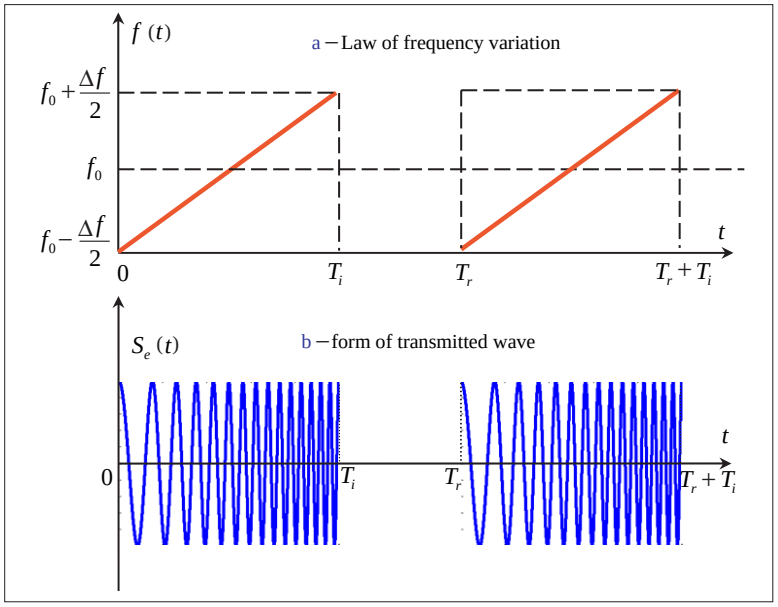

Figure 19. Time variation of the transmitted signal waveform.

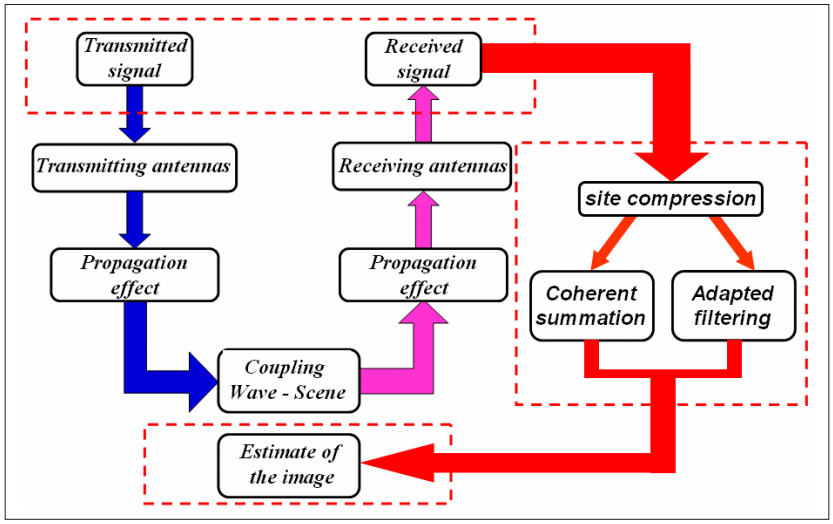

Figure 20. Block diagram of the received signal processing for image reconstruction.

a function of transmitted waveform, transmitting antenna radiation, scattering matrix, and propagation delay. It is expressed in the BSA (*BackScatter Alignment*) convention (Fig. 21) by (33) [5].

$$\vec{E}^r(t) = \begin{bmatrix} E^r_{v_r}(t) \\ E^r_{h_r}(t) \end{bmatrix} = KE_0 \frac{S_r(t)}{c^2 \Delta t_{EC} \Delta t_{CR}} [S(t)][P^e(t)][G^e(t)]\vec{q} \quad (33)$$

Where the received waveform $S_r(t)$ is defined as the waveform of the signal transmitted at time t and delayed from Δt_{ER} such as [17]

$$S_r(t) = S_e(t - \Delta t_{ER}) \quad (34)$$

$[S(t)]$ is the scattering matrix [18], $[P^e(t)]$ is the basis transformation matrix in the transmitting site, $[G^e(t)]$ is the transmitting antenna radiation matrix, and $\vec{q}$ is the transmitting Jones's vector that defines polarization of the transmitting antenna.

The detected voltage at the receiving antenna is obtained by calculating the dot product of the received electric field $\vec{E}^r(t)$ by the effective length $\vec{h}^r_{eff}(t)$ of the receiving antenna. Applying the reciprocity principle, $\vec{h}^r_{eff}(t)$ is similar to the electric field radiated by the antenna if it is used for transmission.

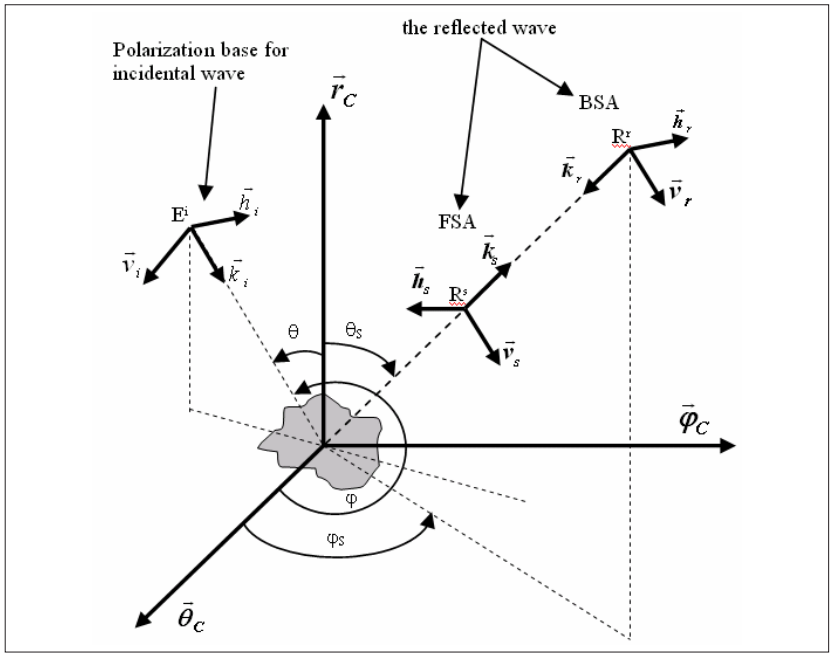

Figure 21. Bistatic scattering configuration.

Then the expression of the detected voltage is given by (35) [16].

$$V_{qp} = KE_0 \frac{S_r(t)}{c^2 \delta t_{EC} \delta t_{CR}} \vec{p}^{*} [G^r(t)]^* [P^r]^* \left[S\left(t - \frac{\delta t}{2} \right) \right] [P^e][G^e(t - \delta t)] \vec{q} \tag{35}$$

Where $\vec{p}$ is the receiving Jones vector that defines polarization of the receiving antenna, $[G^r(t)]$ is the receiving antenna radiation matrix, and $[P^r(t)]$ is the basis transformation matrix in receiving sites.

8. CONCLUSION

In this paper, the signal received by a polarimetric bistatic radar is proposed as a function of time for the general case where the transmitter, the target and the receiver are moving. The signal collected at the receiving antenna is calculated as a function of time, taking into account the vectorial aspect of the electromagnetic waves and various elements operating in the radar radiolink. The received signal is expressed as the voltage detected on the receiving antenna by

taking into account the antenna radiation, the polarimetric behaviour of the target, and the mobile velocity effect. The radar radiolink is designed in a modular structure for a general configuration where the transmitter, the target and the receiver are moving.

The interest of this model is great because it permits, for a defined scenario generation of radar data which can be used in signal processing algorithms for target detection and mapping.

In the companion paper, the received signal by a BISAR presented in this model will be treated by two methods in order to estimate the target reflectivity in the bistatic case. Then, simulation and experimental results will be presented.

REFERENCES

1. D'Errico, M., M. Grassi, and S. Vetrella, "A bistatic mission for earth observation based on a small satellite," *Acta Astronautica*, Vol. 39, Nos. 9–12, 837–846, 1996.
2. Willis, N. J., *Bistatic Radar*, Artech House, Boston London, 1991.
3. Tomiyassu, K., "Bistatic synthetic aperture radar using two satellites," IEEE, 106–110, 1978.
4. Soumekh, M., *Synthetic Aperture Radar Signal Processing*, Wiley-Interscience Publication, United States of America, 1999.
5. Airiau, O. and A. Khenchaf, "A methodology for modeling and simulating target echoes with a moving polarimetric bistatic radar," *Radio Science*, Vol. 35, No. 3, 773–782, May–June 2000.
6. Fitch, J. P., *Synthetic Aperture Radar*, Springer-Verkag, New York, 1988.
7. BenKassem, M. J. and A. Khenchaf, *Bistatic Synthetic Aperture Radar BISAR*, Vol. IV, SCI 2000/ISAS 2000, USA, 2000.
8. Ewell, G. W., "Bistatic radar cross section measurements," *Radar Reflectivity Measurement: Techniques and application*, Currie (ed.), Chap. 5, 139–176, 1989.
9. Hanle, E., "Fundamental problems of bistatic and multistatic radar," *Conference on Modern Radar Problems*, 74–83, Zakopane, Pologne, 1983.
10. Skolnik, M. I., *Radar Handbook*, McGraw-Hill, New York, 1980.
11. Friedrich, K., M. Hagen, and P. Meischner, "Vector wind field determination by bistatic multiple-doppler radar," *Phys. Chem. Earth(B)*, Vol. 25, Nos. 10–12, 1205–1208, 2000.
12. Barton, D. K., C. E. Cook, and P. Hamilton, *Radar Evaluation Handbook*, Artech House, Norwood, MA, 1991.

13. Wong, F. H. and T. S. Yeo "New application of nonlinear chirp scaling in SAR data processing," *IEEE Transactions on Geoscience and Remote Sensing*, Vol. 39, No. 5, 946–953, May 2001.
14. Darricau, J., *Physique et Théorie du Radar*, 3rd ed., Vol. 3, Sodipe, Paris, 1994.
15. Khenchaf, A. and O. Airiau, "Bistatic radar moving returns from sea surface," *IEICE Trans. Electron.*, Vol. E83-C, No. 12, 1827–1835, December 2000.
16. BenKassem, M. J. and A. Khenchaf, "Bistatic mapping radar BISAR," *OCEANS*, San Diego, USA, September 22–26, 2003.
17. Germond, A. L., E. Pottier, and J. Saillard, *Bistatic Radar Polarimetry Theory*, 379–413, CRC Press LLC, 2001.